Indian Journal of Engineering & Materials Sciences
Vol. 30, October 2023, pp. 706-712
DOI: 10.56042/ijems.v30i5.6863

Investigating the Efficiency and Optimization of Germanium-based Perovskite Solar Cell using SCAPS 1D

Anushansha Yadav*, Vanshika, Rahul Kundara, & Sarita Baghel
Department of Applied Physics, Delhi Technological University, Shahbad Daulatpur, New Delhi 110 042, India

Received: *9 August 2023; Accepted*: *26 September 2023*

Germanium-based perovskite solar cells (PSCs) have been a substitute for conventional lead-based perovskite solar cells without sacrificing the environment. In this work, simulation has been carried out with the Cesium germanium bromide, $CsGeBr_3$ perovskite solar Cell on SCAPS-1D and the impact of several factors such as the thickness of the absorber layer, operating temperature and defect density has been analyzed. The device has achieved maximum power conversion efficiency of 11.35 % with an absorber layer thickness of 600 nm at 305 K. The photovoltaic parameters have shown the solar devices to be stable at 305 K. This indicates that $CsGeBr_3$ PSC has become a promising device for future photovoltaic applications and for designing highly efficient lead-free PSC.

Keywords: Absorber, $CsGeBr_3$, Electron transport material (ETL), Hole transport layer (HTL), Heterostructure

1 Introduction

Solar energy has emerged as a highly viable alternative to the energy derived from non-renewable sources in today's society, which has moved toward eco-friendly alternatives for everything. Solar cells have become the gadgets that use the photoelectric effect to convert direct sunlight into electric energy.[1] As a third-generation photovoltaic technology, PSCs have gained prominence because of its advantages of low production costs. The application of perovskite materials in photovoltaic technologies has drawn several scientists and companies. The performance of these devices has not yet been fully tuned, as seen by the variety of topologies, manufacturing techniques, perovskite compositions, and charge selective layers that have been proposed. In a traditional perovskite solar cell, the halogenated compounds function as the active layer. Although these materials have a respectable PCE, their instability and toxicity have been shown to be major drawbacks. Lead-based perovskite solar cells are harmful for the environment, thus numerous alternatives have been employed in their stead, including Ti, Ge, Sn, Sb, and Bi. There are two ways to lessen the toxicity of the solar cell: the first is to substitute lead with an analogous element, and the second is to replace lead with a tin-lead alloyed perovskite ($CH_3NH_3Sn_xPb_{1-x}$).[2,3] As a result, lead-free perovskite materials including those based on Sn and Ge have grown in popularity. However, Sn-based perovskite solar cells still have certain drawbacks, including: (1) Volatile in naturalistic environments; (2) Sn^{2+} is quickly oxidized to Sn^{4+}. As a member of the same family as tin and lead, germanium (Ge)-based perovskite solar cells have gained popularity[4] among researchers. Germanium's band gap is an ideal value for light harvesting, and it has been discovered that halides of germanium are stable at 150°C.[5] Because of its inherent polarity, non-centrosymmetric crystal structure, bandgap of 2.38 eV which offers a significant visible light absorption and photo responses, and distorted crystallinity, cesium germanium tribromide ($CsGeBr_3$) has been a remarkable material for use as an absorbing layer in solar cells. The $CsGeBr_3$ PSC has been simulated using the SCAPS software. SCAPS is a program for numerically simulating solar cells using a range of semiconductor topologies.[6,7] The HTL and ETL layers as well as the cell's thickness, defect density and temperature have all been optimized in this work using SCAPS software.

2 Materials and Methods

2.1 Structure of Perovskite Solar Cell

A perovskite solar cell (PSC), is a type of solar cell that utilizes perovskite material in its operational mechanism. The fundamental structure of a perovskite solar cell consists of several layers: substrate, TCO layer, hole transport layer, perovskite layer, electron

*Corresponding author (E-mail: anuy9168@gmail.com)

transport layer, and back electrode. The substrate serves as the bottom layer of the cell, providing support for the other layers while also absorbing light and generating electricity. Above the active layer, a thin layer of electron transport material (ETM) is applied, facilitating the movement of negative charge carriers from the absorber layer to the back contact. The back electrode, situated at the rear of the perovskite solar cell, is responsible for collecting the electricity generated. Common materials employed for the back electrode include silver (Ag), aluminum (Al), and gold (Au).

2.2 Simulation

A variety of software were available for solar cell simulations. The one we used for our study is SCAPS (Solar Cell Capacitance Simulator). This software is open source and enabled us to simulate a one-dimensional solar cell. These models were built using just a few simple equations. Hole and electron continuity formulae and the Poisson equation are written as follows:

$$\varepsilon \frac{d^2}{dx^2}\Psi(x) = e\left(-n(x) + p(x) + N_D - N_A + \rho_p - \rho_n\right) \quad \ldots (1)$$

ε represents the permittivity, e represents the electrical charge, p and n represent the concentrations of holes and electrons respectively, which vary depending on the distance x. N_D and N_A denote the concentrations of donors and acceptors respectively, and p and n stand for distribution of holes and electrons.[8]

$$\frac{1}{q}\frac{dJ_n}{dx} = -G_{op}(x) + R(x) \quad \ldots (2)$$

$$\frac{1}{q}\frac{dJ_p}{dx} = G_{op}(x) - R(x) \quad \ldots (3)$$

where J_n and J_p represent the current density of electron and hole, R signifies the total recombination sum of direct and indirect recombination and G_{op} is the optical generation rate. The solutions of Eqs (1)-(3) were obtained under steady state conditions.[9] In our work we carried out a simulation of a proposed solar cell under AM1.5G illumination.

2.3 Proposed structure

The photovoltaic device studied has the following components: Ag (metal back contact)/CuSCN (HTL)/$CsGeBr_3$ (absorbing layer)/C_{60} (ETL)/FTO. Figure 1 depicts the construction of the aforementioned cell structure. Table 1 displays the

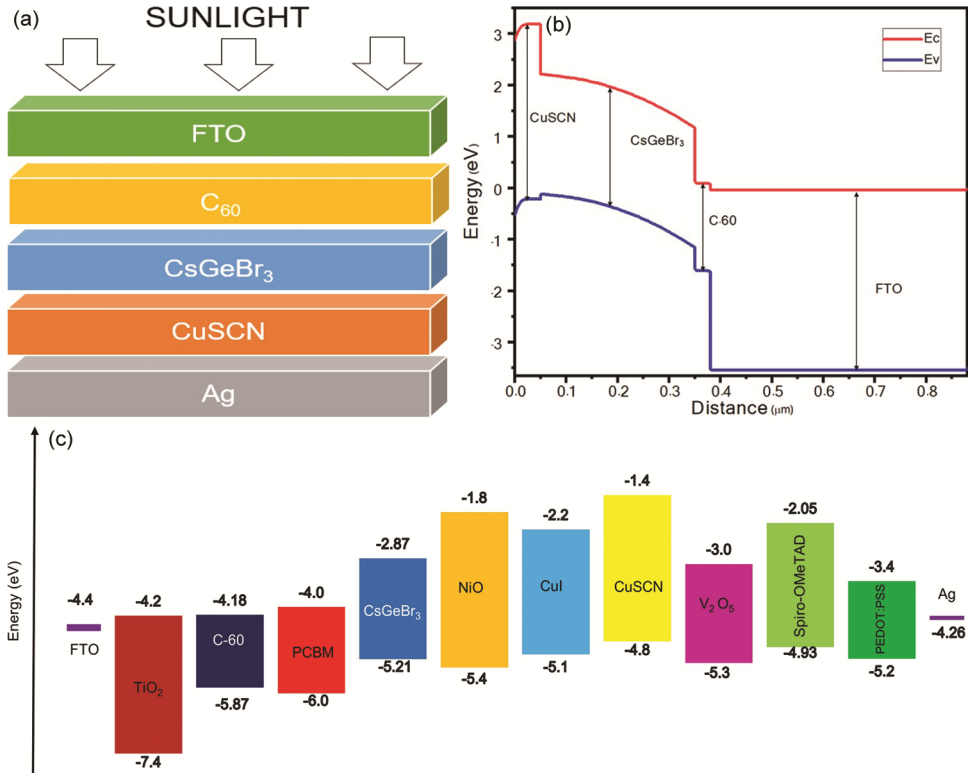

Fig. 1 — (a) Solar cell structure, (b) Energy band diagram of optimized cell layers with contact, & (c) Energy band diagram of different materials without contact.

unique characteristics of $CsGeBr_3$, CuSCN, FTO, and C_{60}, derived from diverse theoretical and experimental investigations documented in the literature.[1, 10-13] A band gap energy of 2.33 eV[11] indicates the outstanding effectiveness of solar cells of $CsGeBr_3$. The early defect density of all materials is assumed to be 1 x 10^{13} cm^{-3}. It is supposed that the thermal velocities of electrons and holes for all the elements used in the cell are 10^7 $cm.s^{-1}$ and 10^7 $cm.s^{-1}$, respectively. The work functions for FTO and Ag are calculated to be 3.5 eV and 4.78 eV, respectively.

Table 1 — Parameters for material used in this simulation

Parameters	FTO	C_{60}	$CsGeBr_3$	CuSCN
Thickness (nm)	500	30	3000	50
Bandgap, E_g (eV)	3.5	1.7	2.33	3.4
Electron affinity (eV)	4	3.9	2.87	1.9
Permittivity	9	4.2	3.9	10
N_c (cm^{-3})	$2.2x10^{18}$	$8x10^{19}$	$1.9x10^{18}$	$1.7x10^{19}$
N_v (cm^{-3})	$1.8x10^{19}$	$8x10^{19}$	$2.07x10^{18}$	$2.5x10^{21}$
Electron Mobility	20	100	20	10^{-4}
Hole Mobility	10	$2.5x10^3$	20	10^{-1}
N_D (cm^{-3})	10^{19}	0	0	0
N_A (cm^{-3})	0	$2.6x10^{18}$	$2x10^{16}$	10^{18}
Defect density	10^{13}	10^{13}	10^{13}	10^{13}

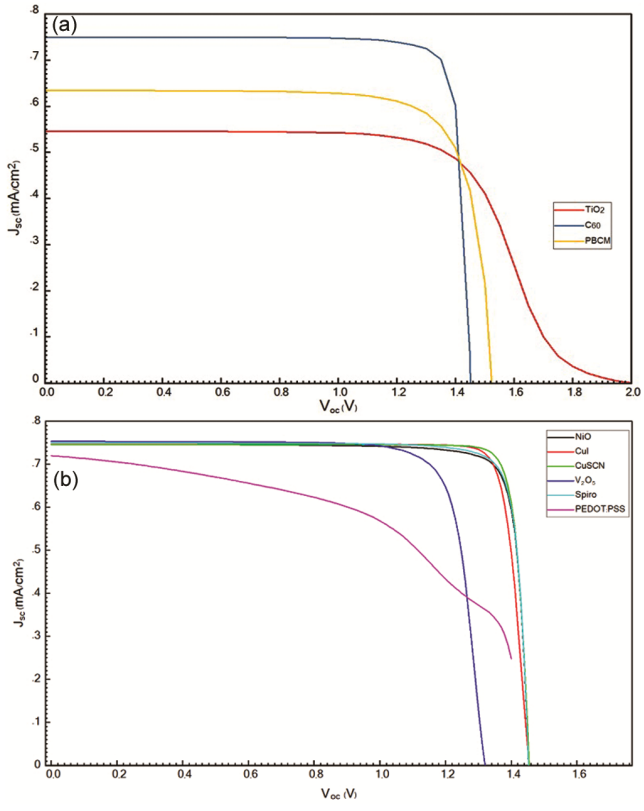

Fig. 2 — Current density (J_{SC}) and voltage (V_{OC}) characteristics of different (a) ETL & (b) HTL materials.

3 Results and Discussions

3.1 Effect of different ETL and HTL combinations on PCE

Cell performance for different cell structures was studied by varying ETL and HTL layers. Fig. 2 & 3 indicate J-V and Q-E characteristics with different HTL and ETL materials, respectively. Table 2 demonstrates the PCE (%) of the solar cell with the different materials used as ETLs and HTLs. From the table it can be seen that the combination of C_{60} (ETL) and CuSCN (HTL) has produced the greatest results in investigations on cell performance with various ETL and HTL layers.

The efficiency of a solar cell that utilizes perovskite light absorbers made of germanium is greatly influenced by the absorber layer. Temperature variations, defect density and the width of the absorber layer all have a considerable effect on the functionality of solar cells. They should be optimized to bring photo-generated electrons and holes into equilibrium, using the names absorption and mixing.[14] First, the thickness is increased from 0.1 μm to 1 μm. We then improved the cell by raising its temperature from 273 K to 423 K using the measurement fit we

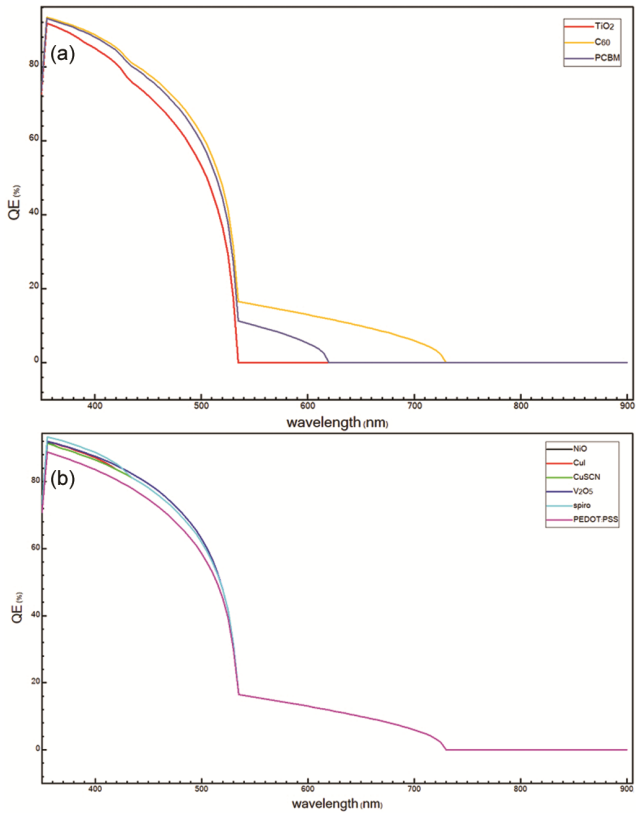

Fig. 3 — Quantum Efficiency QE (%) curve of different (a) ETL, and (b) HTL materials.

Table 2 — Performance of solar cells employing different combinations of various elements as ETLs and HTLs

Cell structures	J_{SC} (mA/cm^2)	V_{OC} (V)	FF (%)	PCE (%)
Ag/NiO/$CsGeBr_3$/TiO_2/FTO	5.40	1.89	66.02	6.76
Ag/CuI/$CsGeBr_3$/TiO_2/FTO	5.41	1.98	67.90	7.29
Ag/CuSCN/$CsGeBr_3$/TiO_2/FTO	5.40	2.15	63.64	7.39
Ag/V_2O_5/$CsGeBr_3$/TiO_2/FTO	5.50	1.59	64.82	5.68
Ag/Spiro-OMeTAD/$CsGeBr_3$/TiO_2/FTO	5.45	1.88	66.77	6.84
Ag/PEDOT:PSS/$CsGeBr_3$/TiO_2/FTO	5.06	1.56	40.17	3.17
Ag/NiO/$CsGeBr_3$/C_{60}/FTO	7.46	1.45	86.99	9.42
Ag/CuI/ $CsGeBr_3$/C_{60}/FTO	7.46	1.45	88.15	9.57
Ag/CuSCN/ $CsGeBr_3$/C_{60}/FTO	7.45	1.45	89.77	9.74
Ag/ V_2O_5/$CsGeBr_3$/C_{60}/FTO	7.53	1.32	81.05	8.06
Ag/Spiro-OMeTAD/ $CsGeBr_3$/C_{60}/FTO	7.50	1.45	87.25	9.50
Ag/PEDOT:PSS/ $CsGeBr_3$/C_{60}/FTO	7.20	1.48	53.81	5.72
Ag/NiO/ $CsGeBr_3$/PCBM/FTO	6.30	1.54	77.72	7.54
Ag/CuI/ $CsGeBr_3$/PCBM/FTO	6.31	1.54	82.18	7.98
Ag/CuSCN/$CsGeBr_3$/PCBM/FTO	6.30	1.55	83.06	8.11
Ag/ V_2O_5/$CsGeBr_3$/PCBM/FTO	6.30	1.54	77.72	7.54
Ag/Spiro-OMeTAD/ $CsGeBr_3$/PCBM/FTO	6.34	1.54	77.88	7.60
Ag/PEDOT:PSS/ $CsGeBr_3$/PCBM/FTO	5.75	1.76	36.83	3.73

found. Next, we changed the defect density of the absorber layer from 10^{12} cm^{-3} to 10^{17} cm^{-3} to get the ideal temperature and thickness of $CsGeBr_3$. We modeled the photovoltaic performance of a Ge-based PSC having an energy gap of 2.33 eV as a function of active layer width, defects and cell temperature. PCE, FF, J_{SC}, and V_{OC} are the characteristics of the device.

3.2 Effect of thickness of absorber layer, $CsGeBr_3$

We see that the J_{SC} value rises with the increase in thickness and reaches the maximum 8.788 mA/cm^2 at thickness of 0.6 μm when the simulation is run for optimizing the absorber layer thickness ranging from 0.1 μm to 1 μm. According to the above statement, it can be inferred that a larger absorber layer has the ability to absorb a greater number of photons. Consequently, this absorption leads to an increased concentration of charge carriers at longer wavelengths, which in turn promotes the production of electron-hole pairs as illustrated in Fig. 4(a). According to Fig. 4(b), an increase in thickness has an impact on V_{OC} values; initially, the V_{OC} slightly rises before becoming almost constant as the thickness rises. As seen in Fig. 4(c), the fill factor falls as the layer becomes thicker. The PCE of the device rises with the extension in width, as shown in Fig. 4(d), and reaches a high of 11.3% at 0.6 μm. With higher charge carrier concentration and more light absorption as a result of increased thickness, J_{SC} values rise due to the material's extremely high absorption coefficient of Ge-based perovskites (up to 105 cm^{-1}).[15] Table 3 shows the optimized device performance values as a function of thickness.

Table 3 — Literature-reported experimental measurements and the optimized results

Parameters	Experimental measurements	Optimized results
J_{SC} (mA/cm^2)	19.49	8.78
V_{OC} (V)	0.48	1.46
FF (%)	52	88.28
PCE (%)	4.92	11.35

3.3 Effect of temperature on $CsGeBr_3$ PSC

The effectiveness of PSCs is significantly affected by temperature. The simulation was run with temperatures ranging from 305 K to 423 K, and it was discovered that 326 K was the ideal temperature when analyzed with a continuous light of 1000 W/m^2. Higher temperature will have an impact on material properties like carrier concentration, band gap energies, and mobility of electron and hole, which will impair cell efficiency.[16] The impact of temperature on J_{SC}, V_{OC}, FF, and PCE is displayed in Fig. 5. As illustrated in Fig. 5 that rise in temperature causes the V_{OC} to fall. Consequently, the influence of temperature on current density is negligible because of the unavoidable drop in voltage. The FF is shown to first rise with temperature before sharply falling. At the point where the perovskite layer is 0.6 μm thick and the temperature is 305 K, the Fill Factor and PCE are at their highest values. The Fig. 5 shows the characteristics for the cell with a band gap of 2.33 eV and a 0.6 μm absorber, such as V_{OC}, J_{SC}, FF, and PCE, with temperatures varies from 305 K to 423 K.

3.4 Effect of defect density on absorber layer

Figure 6 shows how defect density affects every parameter (J_{SC}, V_{OC}, FF and PCE). The graph shows

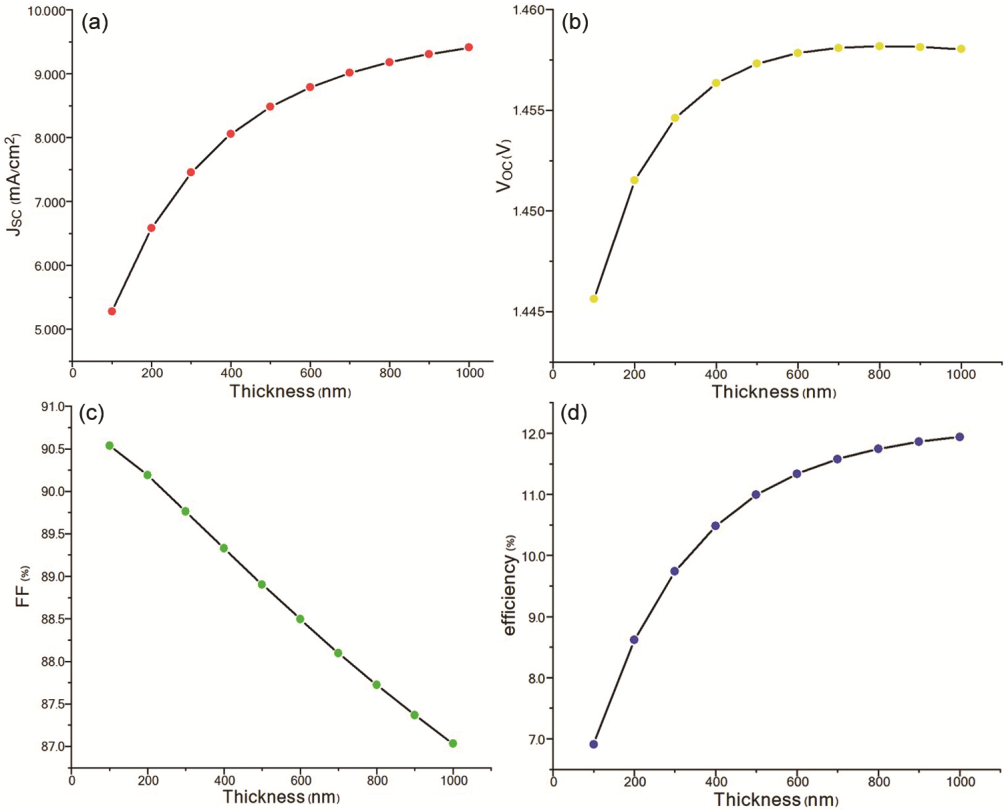

Fig. 4 — Variation in device output parameters due to change in thickness of absorber layer.

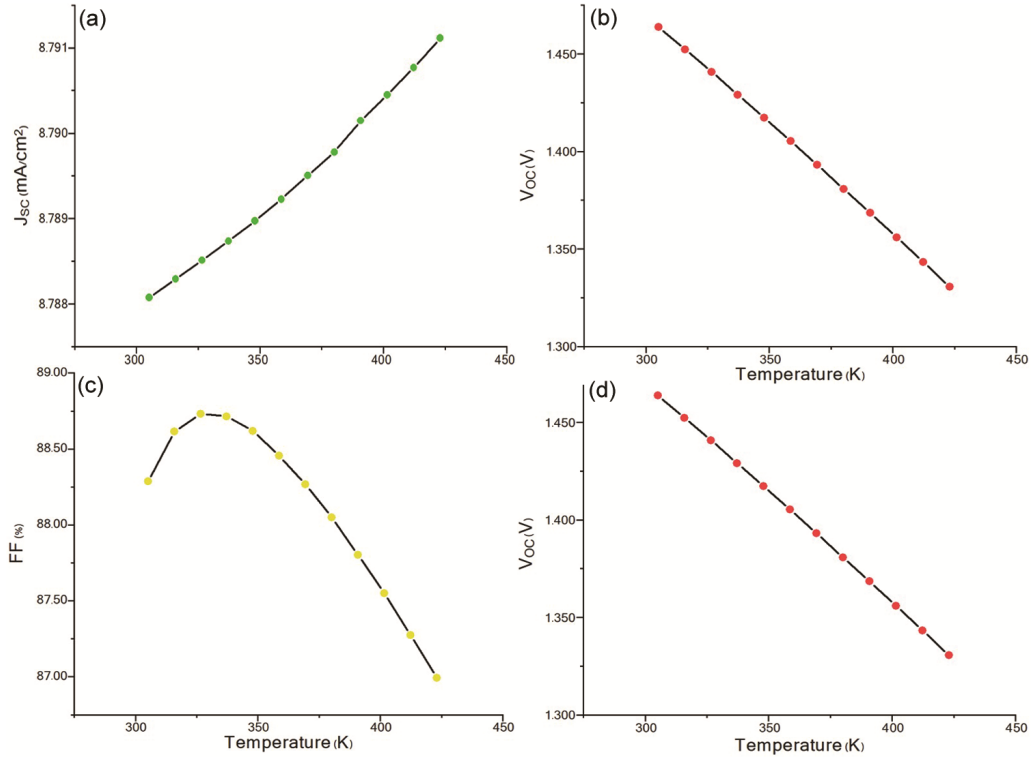

Fig. 5 — Variation in device output parameters due to change in Temperature.

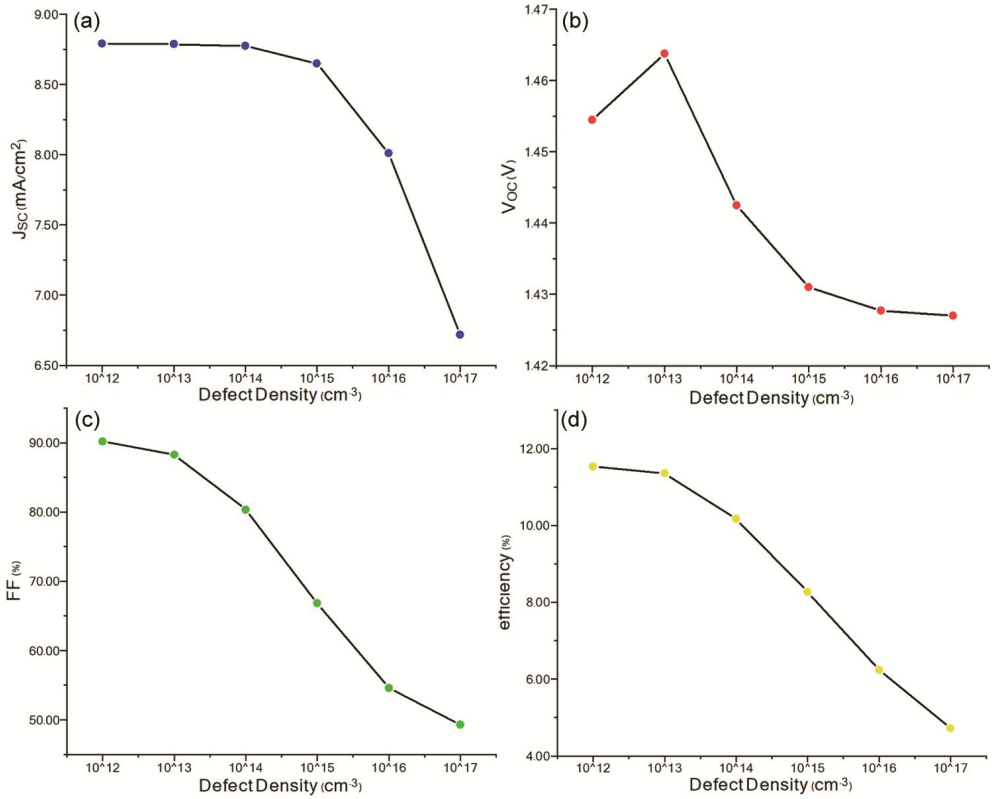

Fig. 6 — Variation in device output parameters due to change in defect density of absorber layer.

that the value of J_{SC} first appears to be practically constant before falling. While the V_{OC} initially rises, then falls, and eventually remains steady. With a rise in the absorber layer's defect density, the fill factor similarly drops. We come to the conclusion that the efficiency is directly impacted by defect density because as defects multiply, charge carriers' diffusion lengths shorten and recombination carriers accumulate in the absorber layer. Fig. 6(d) shows the resulting efficiencies due to variation in the absorber defect density. 10^{13} cm^{-3} is found to be the optimum defect density of the proposed solar cell.

We discover that the effectiveness found in the simulated results is 9.74% using perovskite quantum rods, whereas it was 4.92% in the literature[23], when we compared our findings with the results from the literature. We utilized C_{60} as an ETL in our suggested structure because of its improved electron transporting capabilities, reduction of hysteresis, and low-temperature processing. It can also be packed more tightly to improve inter-molecular charge transmission in addition to these characteristics.[17-19] On the other hand, the use of CuSCN as the HTL in the structure is attributed to its natural thermal stability, exceptional resistance to high temperatures, and an extremely durable crystalline structure. Furthermore, its band alignment with the perovskite is perfect.[20-22] Additionally, the PCE of the outcome has significantly improved in the optimized findings. Table 3 shows the literature - reported experimental measurements and the optimized results obtained in this paper.

4 Conclusion

Our research has focused on examining the influence of various ETLs and HTLs on perovskite solar cells. Our findings have indicated that C_{60} as ETL and CuSCN as HTL have been the most appropriate choices based on their favorable impact. We have investigated how multiple factors, such as operating temperature, absorber layer thickness, and defect density, affect the device parameters, using the SCAPS-1D simulation. The simulation result has shown that the maximum PCE of 11.35% has been attained for the device structure Ag/CuSCN/$CsGeBr_3$/C_{60}/FTO at a thickness of 600 nm. The optimized value of temperature and defect density of the PSC is 305 K and 10^{13} cm^{-3} respectively. The proposed structure after optimization has shown excellent results in PCE when compared to the work done in literature.

Acknowledgement

We are grateful to the Delhi Technological University for catering our work and to our batchmates for informative discussions.

References

1 Chakraborty K, Choudhury M G, Paul S, *Solar Energy*, 194 (2019) 886.
2 Ogomi Y, Morita A, Tsukamoto S, Saitho T, Fujikawa N, Shen Q, Toyoda T, Yoshino K, Pandey S S, Ma T, Hayase S, *J Phys Chem Lett*, 5 (2014) 1004.
3 Hao F, Stoumpos C C, Chang R P H, Kanatzidis M G, *J Am Chem Soc,* 136 (2014) 8094.
4 Zhang Q, Hao F, Li J, Zhou Y, Wei Y, Lin H, *Sci Technol Adv Mater*, 19 (2018) 425.
5 Meng X, Tang T, Zhang R, Liu K, Li W, Yang L, Song Y, Ma X, Cheng Z, Wu J, *Opt Mater (Amst)*, 128 (2022).
6 Sarker S, Islam MT, Rauf A, Al Jame H, Jani MR, Ahsan S, Islam M S, Nishat S S, Shorowordi K M, Ahmed S, *Solar Energy*, 225 (2021) 471.
7 Et-taya L, Ouslimane T, Benami A, *Solar Energy*, 201 (2020) 827.
8 Nalianya MA, Awino C, Barasa H, Odari V, Gaitho F, Omogo B, Mageto M, *Optik (Stuttg),* 248 (2021).
9 E.H. Youssef, A. Benami, Investigation of the effect of thickness, band gap and temperature on the efficiency of CIGS solar cells through SCAPS-1D, 109 International Journal of Engineering and Technical Research. 22 (2016) 2454–4698. www.erpublication.org (accessed April 3, 2023).
10 Jong U G, Yu C J, Kye Y H, Choe Y G, Hao W, Li S, *Inorg Chem*, 58 (2019) 4134.
11 Han N T, Dien V K & Lin M F, *ACS omega*, 7 (2022) 25210.
12 Saikia D, Alam M, Bera J, Betal A, Gandi AN, Sahu S, *Adv Theory Simul*, 5 (2022).
13 U. Jonga, C. Yu, Y. Kye, Y. Choe, … H.W. preprint arXiv, undefined 2018, Structural and optoelectronic properties of the inorganic perovskites AGeX3 (A= Cs, Rb; X= I, Br, Cl) for solar cell application, Arxiv.Org. (2018). https://arxiv.org/abs/1810.02543 (accessed April 3, 2023).
14 Zhao P, Liu Z, Lin Z, Chen D, Su J, Zhang C, Zhang J, Chang J, Y. Hao, *Solar Energy*, 169 (2018) 11.
15 Sun P P, Li Q S, Yang L N, Li Z S, *Nanoscale*, 8 (2016) 1503.
16 Chen J, Shen H, Zhai Z, Li J, Wang W, Shang H, Li Y, *Journal of Physics D Applied Physics*, 49 (2016) 495601.
17 Liu X, Liu Z, Ye H, Tu Y, Sun B, Tan X, Shi T, Tang Z, Liao G, *Electrochim Acta*, 288 (2018) 115.
18 Zhou H, Mei J, Xue M, Song Z, Wang H, *Journal of Physical Chemistry C,* 121 (2017) 21541.
19 Xu C, Zhang Y, Luo P, Sun J, Wang H, Lu Y W, Ding F, Zhang C, Hu J, *ACS Appl Energy Mater,* 4 (2021) 5543.
20 Jung M, Kim Y C, Jeon N J, Yang W S, Seo J, Noh J H, Seok S Il, *ChemSusChem*. 9 (2016) 2592.
21 Mahapatra B, Krishna R V, Laxmi, Patel P K, *Opt Commun,* 504 (2022).
22 Nizamuddin A, Arith F, Rong I J, Zaimi M, Rahimi A S, Saat S, *Journal of Advanced Research in Fluid Mechanics and Thermal Sciences*, 78 (2021) 153.
23 L.C.-R. advances, undefined 2018, Synthesis and optical properties of lead-free cesium germanium halide perovskite quantum rods, Pubs.Rsc.Org. (n.d.). https://pubs.rsc.org/en/content/articlehtml/2018/ra/c8ra01150h (accessed April 3, 2023).